Journal of the Meteorological Society of Japan, Vol. 90B, pp. 33–45, 2012
doi:10.2151/jmsj.2012-B03

Numerical Simulation of Urban Heat Island Effect by the WRF Model with 4-km Grid Increment: An Inter-Comparison Study between the Urban Canopy Model and Slab Model

Hiroyuki KUSAKA

Center for Computational Sciences, University of Tsukuba, Tsukuba, Japan

Fei CHEN, Mukul TEWARI, Jimy DUDHIA, David O. GILL, Michael G. DUDA, Wei WANG

National Center for Atmospheric Research, Boulder, CO, USA

and

Yukako MIYA

Graduate School of Life and Environmental Sciences, University of Tsukuba, Tsukuba, Japan

(Manuscript received 4 July 2011, in final form 22 December 2011)

Abstract

The present study applies the WRF model involving the single-layer urban canopy model (hereafter, WRF_UCM) to urban climate simulation of the Tokyo metropolitan area for August (2004–2007) and compare results to (a) observations, and (b) the WRF model involving the slab urban model (hereafter, WRF_SLAB). In this urban area, WRF_UCM accurately captures the observed monthly mean daytime and nocturnal UHI, whereas WRF_SLAB does not show a nocturnal UHI. Moreover, the observed diurnal variations of the surface air temperature for central Tokyo and Kumagaya, a nearby inland city, are reproduced well by WRF_UCM. However, WRF_SLAB exhibits both a 1-hr phase shift and a 6.2°C excess oscillation magnitude over observations. In addition, WRF_UCM accurately reproduces the frequency distribution of surface air temperatures, showing a maximum at 27°C, whereas WRF_SLAB produce a bimodal distribution, with double peaks at 23 and 33°C. Finally, WRF_UCM does a much better job than WRF_SLAB at modeling the relative humidity.

1. Introduction

The surface layer in cities is generally warmer than that of the surrounding areas, a phenomenon known as the urban heat island (UHI) effect. UHI effects are stronger under clear skies and light winds during nighttime, with the largest impact occurring in winter. Thus, most of the early studies focused on the nocturnal UHI in winter (Yoshino 1975, Landsberg 1981, Oke 1987). Recently, the summertime UHI has become a serious health and economic concern in Japan due to the associated higher average temperatures. For example, the number of deaths caused by heat stroke has more than doubled in recent years, now exceeding the deaths from other weather disasters, including typhoons and tornados (Fujibe 2009). Ambulances transport more than 10,000 people with heat stroke to the hospitals in the Tokyo metropolitan area in summer (Fire and Disaster Management Agency of Japan 2011). Moreover, gaining a better understanding of the UHI in Japan is important because an increase in the daytime high by 1°C in summer increases daily maximum energy demand by about 1,900,000 kW in the Tokyo metropolitan area and

Corresponding author: Hiroyuki Kusaka, Center for Computational Sciences, University of Tsukuba, Tsukuba, 305-8572, Japan.
E-mail: kusaka@ccs.tsukuba.ac.jp

its surroundings, as a result of increased air-conditioning demand (e.g., Goto et al. 2004). Also, sleep disruption is common in summer, which leads to an associated economic loss during business hours (Ihara et al. 2011). Thus, many Japanese cities require the mitigation of the UHI effect.

Projection of social implications of the future UHI is a concern for both impact assessment researchers and urban residents. These concerns can be addressed using an urban canopy model (UCM) coupled to a larger-scale atmospheric and climate model. In the urban climate study fields, a number of UCM schemes have been developed (e.g., Brown and Williams 1998, Masson 2000, Kusaka et al. 2001, Martilli et al. 2002, Harman et al. 2004, Otte et al. 2004, Kondo et al. 2005, Best 2005, Kanda et al. 2005, Lee and Park 2008, Oleson et al. 2008, Ikeda and Kusaka 2009, Porson et al. 2009, 2010, Aoyagi and Seino 2011). Some researchers have coupled a UCM to a global climate model (GCM) (McCarthy et al. 2010, Oleson et al. 2011), and others couple the UCM to a regional climate model (RCM) (e.g., Lemonsu and Masson 2002, Rozoff et al. 2003, Dupont et al. 2004, Otte et al. 2004, Dandou et al. 2005, Holt and Pullen 2007, Zhang et al. 2007, Chen et al. 2010, Aoyagi and Seino 2011).

The Weather Research and Forecasting (WRF) model (Skamarock et al. 2008), a regional atmospheric model, has been recently used in the urban climate field world-wide since the single-layer UCM (Kusaka et al. 2001) was installed (e.g., IAUC 2009, Chen et al. 2010). Performance of the WRF model with the single-layer UCM has been already evaluated in many case studies with regards to the UHI and urban boundary layer structure. Miao et al. (2009) used the WRF with the single-layer UCM to simulate the UHI and boundary layer structures in Beijing, and showed that the model could reproduce the observed diurnal variation of UHI intensity, the spatial distribution of UHI, the diurnal variation of wind speed and direction, and small-scale boundary layer convective rolls and cells over the urban area. Later, Chen et al. (2011) applied this modeling system to the Houston-Galveston area, and found that it did a remarkable job of capturing the observed nocturnal UHI intensity, diurnal rotation of surface winds, as well as the timing and vertical extent of the sea breeze and its reversal in the boundary layer. Lin et al. (2008), Shou and Zhang (2010), and Chen et al. (2011) investigated the interaction between UHI and sea breeze. Miao et al. (2010, 2011) and Lin et al. (2011) evaluated the impact of urbanization on heavy rainfalls. Grossman-Clarke (2010) examined the contribution of land-use changes to surface air temperatures during an extreme heat events in the Phoenix metropolitan area. Takane and Kusaka (2011) examined the record-breaking extreme high surface air temperature observed in the Tokyo metropolitan area and showed the utility of this modeling system for studying foehn and UHI phenomena. Jiang et al. (2008) predicted impacts of land use change on surface ozone in the Houston. Tewari et al. (2010) used the WRF model and CFD model for urban scale contaminant transport and dispersion simulation. Miao et al. (2010) and Zhang et al. (2010) showed that the WRF model coupled to the single-layer UCM could reproduce the monthly-average UHI over the Beijing and the Yangtze River Delta Economic Belt areas. In this study, we use the WRF model with a single-layer UCM to simulate August surface temperatures and humidities in the Tokyo metropolitan area. Our primary purpose is to evaluate the reproducibility of UHI and relative humidity (RH) observations. Moreover, to provide useful information for numerical model developers, we compare results on the UHI and RH from coupling the WRF model to two urban models: the UCM model and the often-used, traditional slab urban model (SLAB). The comparison also provides useful information to agencies tasked with safety or power services.

2. Description of the numerical simulation and urban models

We used the WRF-ARW model, version 3.0.1.1, to simulate the summertime urban climate over the Tokyo metropolitan area. The present simulations are a type 2 dynamic downscaling summarized by Castro et al. (2005) in which the initial atmospheric conditions have been forgotten, but results still depend on the lateral boundary conditions from global data analysis and on the bottom boundary conditions. The model domain covers central Japan, including the Tokyo metropolitan area. As shown in Fig. 1, the Tokyo metropolitan area is surrounded by the Pacific Ocean and the Chubu mountains. For these experiments, the nominal horizontal grid spacing in the WRF model is 4 km. The model top is set to be 50 hPa, with 35 vertical σ-levels. The time integration covers from July 27th to September 1st for four consecutive years (2004–2007), referred to here as four consecutive Augusts.

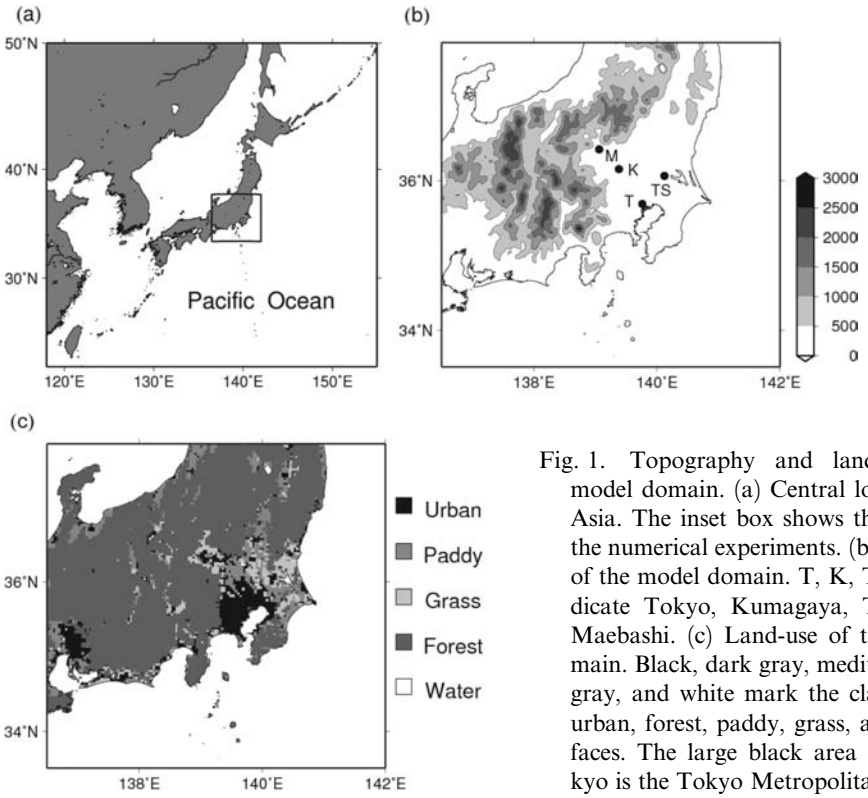

Fig. 1. Topography and land-use of the model domain. (a) Central location within Asia. The inset box shows the domain for the numerical experiments. (b) Topography of the model domain. T, K, TS, and M indicate Tokyo, Kumagaya, Tsukuba, and Maebashi. (c) Land-use of the model domain. Black, dark gray, medium gray, light gray, and white mark the classification of urban, forest, paddy, grass, and water surfaces. The large black area including Tokyo is the Tokyo Metropolitan Area.

Each month is a single simulation. The first four days of each simulation are discarded and considered as the model spin-up.

The atmospheric initial and boundary conditions are created from 6-hourly Japan Meteorological Agency-Regional Analysis data (JMA-RANAL) with 20-km horizontal grid spacing. The land state input is provided by the 6-hourly National Center for Environmental Prediction-Final Analysis data (NCEP-FNL) with 1.0° horizontal grid spacing. The sea surface temperature field comes from the daily NCEP-Real Time Global Sea Surface Temperature analysis data (NCEP-RTG_SST) with 0.5° horizontal grid spacing. Our land-use categories and terrain-height datasets came from the Geospatial Information Authority of Japan.

The simulation uses the following physics schemes: the Dudhia short-wave radiation scheme, a simple integration scheme that efficiently treats clouds and clear-sky absorption and scattering (Dudhia 1989); the Rapid Radiative Transfer Model (RRTM) for long-wave radiation, which accounts for multiple bands, trace gases, and microphysics species (Mlawer et al. 1997); the WRF Single-Moment 6-class (WSM6) microphysics scheme, a cold-rain model with water vapor, cloud, rain, ice, snow, and grauple processes (Hong et al. 2004); the Yon-Sei University (YSU) planetary boundary layer scheme, a non-local turbulent diffusion scheme with an explicit entrainment layer and parabolic diffusion coefficient profile in an unstable mixed layer (Hong and Pan 1996, Hong et al. 2006); the Kain-Fritsch cumulus parameterization scheme for the parent domain (Kain and Fritsch 1990). Because of the 4-km horizontal grid spacing, we use no Kain-Fritsch cumulus parameterization scheme in the inner domain. For a land-surface model, the UCM case uses the Noah land surface model (Noah-LSM) (Chen and Dudhia 2001) coupled with a single-layer UCM (Kusaka et al. 2001, Kusaka and Kimura 2004a, b), whereas the SLAB case uses the 5-layer thermal diffusion model (historically called the SLAB model in WRF). Except for the land-surface model, all configurations for SLAB case are the same as those for UCM case. Model configurations are summarized in Table 1.

The single-layer UCM used in the WRF model was developed by Kusaka et al. (2001), and later modified by Kusaka and Kimura (2004a, b) and

Table 1. Model configuration.

Model	ARW-WRF Version 3.0.1.1
Shortwave Radiation	Dudhia
Longwave Radiation	RRTM
Cloud Microphysics	WSM6
Cumulus Parameterization	-----
Planetary Boundary Layer	YSU
Land surface	Slab 5-layer (case SLAB) Noah coupled with UCM (case UCM)
Initial and Boundary Conditions	Japan Meteorological Agency-Regional Analysis (Atmosphere), NCEP-Final Analysis (Soil), NOAA-RTG SST (SST)
Simulation Period	00 UTC 27 July to 00 UTC 1 September, 2004, 2005, 2006, 2007
Horizontal Grid Spacing	4 km
Total Number of Vertical Layers	35

Miao et al. (2009). The model includes street canyons that are parameterized to represent the urban geometry and a multi-layer heat equation for the roof, wall, and road interior temperatures. The UCM case estimates both the surface temperatures of, and the heat fluxes from, the roof, wall, and road (Fig. 2). (For more details on the single-layer UCM, see Kusaka et al. (2001) and Kusaka and Kimura (2004a, b).) In the WRF model, the single-layer UCM couples with the Noah-LSM.

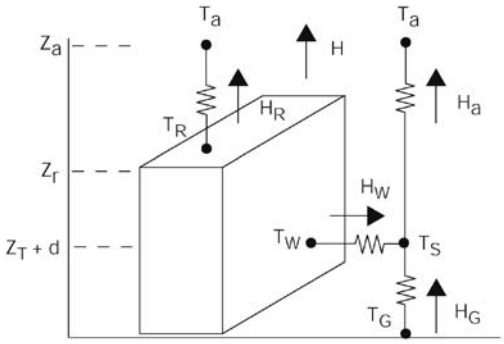

Fig. 2. Temperatures and heat fluxes in the single-layer UCM. T_a is the air temperature at reference height z_a, T_R the building roof temperature, T_W the building wall temperature, T_G the road temperature, and T_S the temperature at height $z_T + d$. H is the sensible heat exchange at the reference height. H_a is the sensible heat flux from the canyon space to the atmosphere, whereas H_W is that from wall to the canyon space, H_G is that from the road to the canyon space, and H_R is that from the roof to the atmosphere.

Surface fluxes from artificial and natural surfaces in the WRF model grid are calculated from the UCM and the Noah-LSM, respectively. Then, total fluxes from the model grid are calculated using a sub-grid parameterization for heterogeneous surfaces, as proposed by Kimura (1989). (For more details on the coupled Noah-LSM and UCM system, see Chen et al. (2011).) The UCM uses the anthropogenic heat-emission data shown in Fig. 3. For the Tokyo metropolitan area, the area-averaged, daily-mean anthropogenic heat is assumed to be 18 W m^{-2}. Other parameters for the UCM are listed in Table 2.

The SLAB model consists of the standard surface layer scheme based on the Monin-Obukhov similarity theory for estimating bulk transfer coefficients, a surface heat budget equation for simulating surface skin temperature, and a vertical diffusion equation for simulating soil temperature. Urban geometry is represented by tuning surface parameters such as roughness length, albedo, thermal inertia, and moisture availability. However, anthropogenic heat emission is not considered in

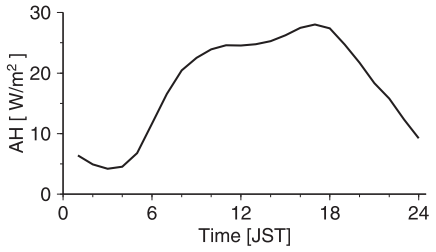

Fig. 3. Diurnal cycle of the anthropogenic heat emission in the UCM.

Table 2. Parameters used in the UCM model. The value in parentheses is gross building coverage ratio.

Parameter	Value
Green fraction [−]**	0.3
Building height [m]	9.0
Building coverage ratio [−]**	0.35 (0.245*)
Sky view factor [−]**	0.59
Thermal Inertia [J s^{-1} K^{-2} m^{-4}]	3.52×10^6

* Gross building ratio.
** Dimensionless.

Table 3. Parameters used in the SLAB model.

Parameter	Value
Roughness Length [m]	0.80
Moisture Availability [−]*	0.10
Albedo [−]*	0.15
Emissivity [−]*	0.88
Thermal Inertia [J s^{-1} K^{-2} m^{-4}]	3.0×10^6

* Dimensionless.

this model. This type of model has been widely used because of its simplicity. For this study, we used the default parameters settings listed in Table 3.

Hereafter, the experiments with the WRF model involving the single-layer UCM and SLAB are called UCM and SLAB, respectively.

3. Results

3.1 Surface air temperature

a. Spatial distribution in the analysis domain

We compare surface air temperatures from the WRF model simulations against data from the Japan Meteorological Agency's (JMA) Automated Meteorological Data Acquisition System (AMeDAS) network. To account for the difference in the terrain height between the model grid and the observation site, we assume a temperature lapse rate of -0.0065°C m^{-1}.

Figure 4 compares the error distribution from UCM and SLAB cases. The error distribution of the entire domain is roughly normally distributed for the both models. The bias and RMSE over the entire domain for SLAB are −0.6°C and 2.5°C, respectively (Table 4). On the other hand, the bias and RMSE for UCM are −0.4°C and 2.1°C, respectively.

Figure 5 shows the spatial distribution of the monthly mean surface air temperature at 0500 Japan Standard Time (JST). SLAB does not reproduce the observed UHI, largely underestimating the temperature in the Tokyo metropolitan area (Figs. 5a,b). In contrast, UCM simulates UHI, although the model overestimates the temperature over this region (Figs. 5a,c). UCM has a smaller bias and RMSE than SLAB (Table 4). At 1500 JST, SLAB and UCM give the observed tempera-

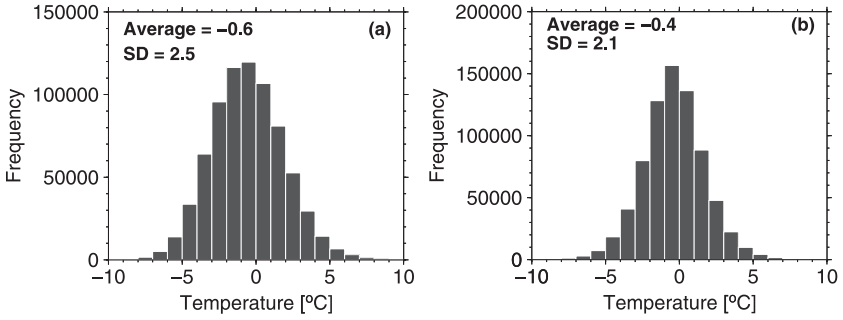

Fig. 4. Error distribution of the surface air temperature over the entire analysis domain from (a) SLAB and (b) UCM.

Table 4. Surface temperature bias [°C] and RMSE [°C] over the entire analysis domain at indicated times. Values for just the urban areas are in parentheses.

	Bias	RMSE	Bias at 05 JST	RMSE at 05 JST	Bias at 15 JST	RMSE at 15 JST
SLAB	−0.6 (−0.3)	2.5 (2.8)	−2.0 (−2.6)	3.1 (3.3)	+0.6 (+1.8)	2.4 (2.8)
UCM	−0.4 (+0.7)	2.1 (1.8)	−0.1 (+1.0)	2.0 (1.8)	−0.8 (+0.4)	2.4 (2.0)

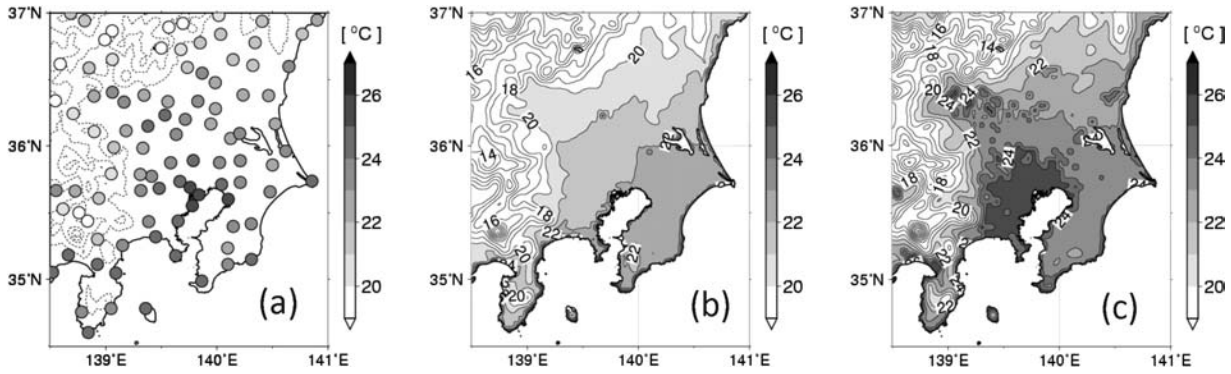

Fig. 5. August mean surface air temperature [°C] at 0500 Japan Standard Time (JST) for 2004–2007 from (a) AMeDAS observations, (b) SLAB, and (c) UCM.

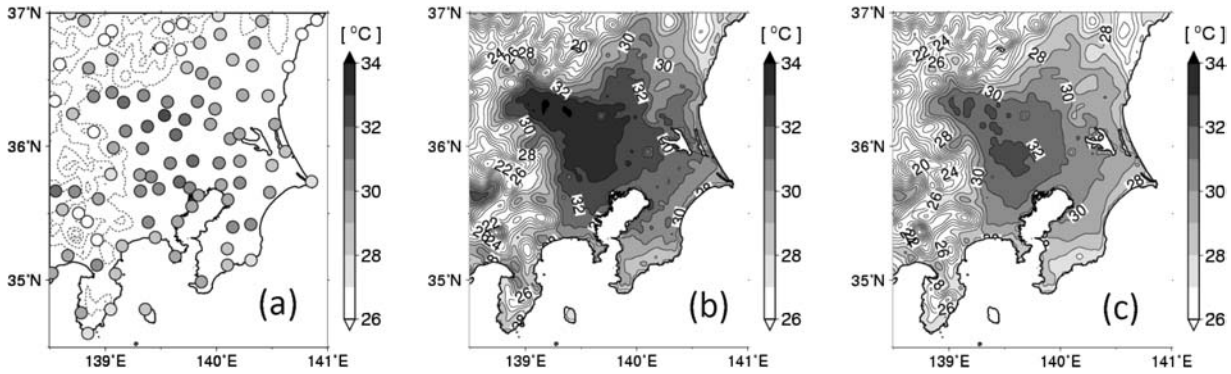

Fig. 6. Same as Fig. 5, but for 1500 JST.

ture distribution but they overestimate the temperature in the northwestern inland areas (Fig. 6). For SLAB, the overestimate is about 2°C, but less than 1°C from UCM. As a result, the bias from SLAB exceeds that from UCM over the urban areas at 1500 JST, as shown in Table 4. The table also shows that the RMSE from SLAB is comparable to that from UCM, over both the analysis domain and the urban areas.

b. Coastal mega-city Tokyo and inland medium-city kumagaya

In this sub-section, we focus on the coastal mega-city of Tokyo and the inland medium-sized-city Kumagaya that is located in the northwest portion of the Tokyo metropolitan area, 62-km northwest of the Tokyo station. Due partly to its urbanization, climate change, and the feohn phenomena, the latter city had the high-temperature record of 40.9°C for Japan (Takane and Kusaka 2011).

The AMeDAS network consists of two types of observatories; one is AMeDAS, which was established for predicting and monitoring weather associated with disasters, whereas the other platform is the original, more established, JMA observatories. The JMA sites have relatively large, open-space, covered with short grasses, and adhere to stricter installation standards. Consequently, JMA stations are desirable from a standpoint of model-evaluation.

Figure 7a shows the AMeDAS network data at Otemachi observatory in downtown Tokyo, (hereafter Tokyo), and the two model cases. SLAB has an excess diurnal range of nearly 6.2°C over the observations as well as a 1-hr temporal shift. The diurnal variation from UCM more closely matches

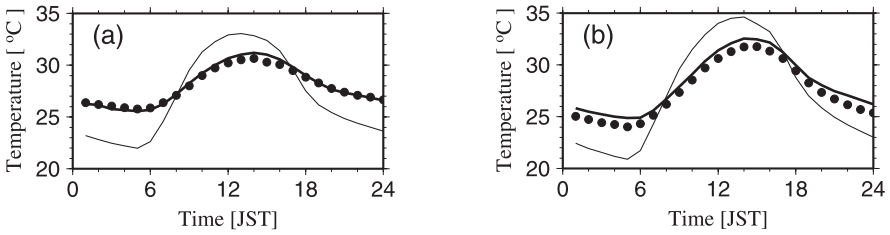

Fig. 7. Diurnal variations of surface air temperature [°C] at (a) Tokyo and (b) Kumagaya. Monthly mean temperature for each hour in August for 2004–2007. Solid circles are observations. Thin and thick solid lines are results from SLAB and UCM.

Table 5. Model bias of surface temperature [°C] at the JMA observatories. RMSE values are in parentheses. TO, KU, MA, TS, UT, CHO, CHI, TA, and YO are city locations described in Table A1.

	TO	KU	MA	TS	UT	CHO	CHI	TA	YO
SLAB	−0.9 (3.1)	−0.2 (3.1)	−0.1 (3.1)	+0.4 (2.5)	−0.1 (3.0)	+0.6 (2.2)	−0.7 (2.5)	−0.5 (1.7)	−0.6 (2.0)
UCM	+0.1 (1.3)	+0.7 (1.8)	+0.8 (1.9)	+0.7 (1.7)	−0.5 (1.6)	+0.9 (1.7)	+0.3 (1.9)	−0.2 (1.4)	−0.2 (2.0)

observations and shows no discernable phase lag. These same features also occur at Kumagaya (Fig. 7b).

The frequency distribution of observed and simulated hourly surface air temperatures are shown in Fig. 8. In Tokyo, the observations show only one peak around 27°C, whereas SLAB has two maxima, located at approximately 23 and 33°C (Figs. 8a,b). The RMSE is 3.1°C for SLAB (Table 5). The weighted mean value of the temperature in the histogram is 27.9°C in the observations, but 27.0°C in SLAB, implying a temperature bias of −0.9°C. Nevertheless, because of its bimodal distribution, SLAB greatly overestimates the number of abnormally hot days in Japan (i.e., maximum exceeding 35°C). At Kumagaya, similar to Tokyo, SLAB shows a bimodal shape, which contrasts to the single-peaks in the AMeDAS data (Figs. 8d,e).

In contrast, the frequency distribution of hourly surface air temperatures in UCM closely matches observations at Tokyo (Figs. 8a,c). RMSE from the UCM is 1.3°C and the temperature bias is +0.1°C, which are much smaller than those in SLAB (Table 5), although UCM has more temperature of 25°C than the observations. Similar to that for Tokyo, at Kumagaya the shape of the histogram and RMSE from UCM match the observations much better than those from SLAB (Figs. 8d,f, Table 5). Of course, there are some discrepancies with the observations; the UCM model hardly produces low temperature below 18°C or high temperature exceeding 36°C. Although SLAB produces smaller overall surface air-temperature bias than UCM due to the compensating errors described above, the temperature RMSE in UCM is lower than that in SLAB.

In the UCM, the interannual variability of the monthly averaged surface air temperatures is also better captured than SLAB (Fig. 9). In Tokyo, UCM fits the oscillations of the monthly mean, maximum, and minimum temperatures (Fig. 9a). Not only does SLAB have maxima that are too warm and minima that are too cold, SLAB also does not follow the general trend of the interannual oscillations, especially the minimum temperature. The large minimum temperature errors, even in the urbanized site, imply that the nocturnal cooling is too strong in the SLAB model. At Kumagaya, the overall results for the interannual surface air temperature are similar to those from Tokyo (Fig. 9b), except UCM fails to follow the temperature oscillation in 2004 due to the model's behavior with a positive temperature bias. Nevertheless, for Kumagaya, UCM has a smaller amplitude bias and generally fits observations better than SLAB.

3.2 Relative humidity

As with the temperature distributions, UCM more accurately reproduces the frequency distributions for the hourly RH than SLAB (Fig. 10). For Tokyo, the shape of the histogram from SLAB clearly differs from that of the AMeDAS observa-

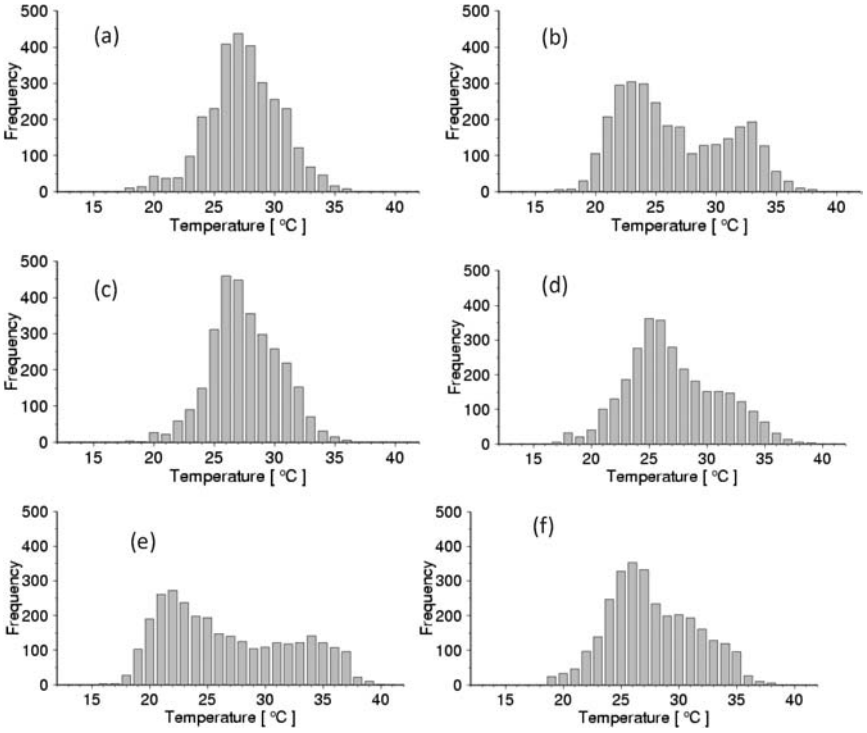

Fig. 8. Frequency of surface air temperatures [°C] at Tokyo and Kumagaya in August for 2004–2007. (a) AMeDAS observations at Tokyo, (b) SLAB at Tokyo, (c) UCM at Tokyo, (d) AMeDAS observations at Kumagaya, (e) SLAB at Kumagaya, and (f) UCM at Kumagaya.

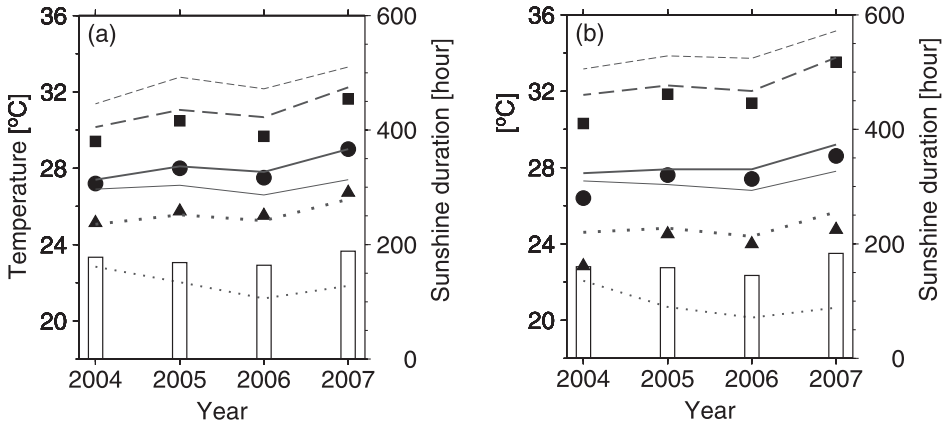

Fig. 9. Interannual variation of the monthly temperatures and monthly cumulative hours of sunshine duration at (a) Tokyo and (b) Kumagaya. Closed circles, squares, and triangles are the observed mean, maximum, and minimum temperatures, respectively. Thick solid, dashed, and dotted lines are the mean, maximum, and minimum temperatures from UCM, respectively. The corresponding thin lines are from SLAB. White bars show the observed monthly accumulated sunshine duration.

tions (Figs. 10a,b), whereas that from UCM agrees fairly well with the observations (Figs. 10a,c). Indeed, the bimodal shape of the SLAB distribution arises from that of the surface-temperature distribution. Similarly, for the frequency distribution at Kumagaya, UCM produces better results than

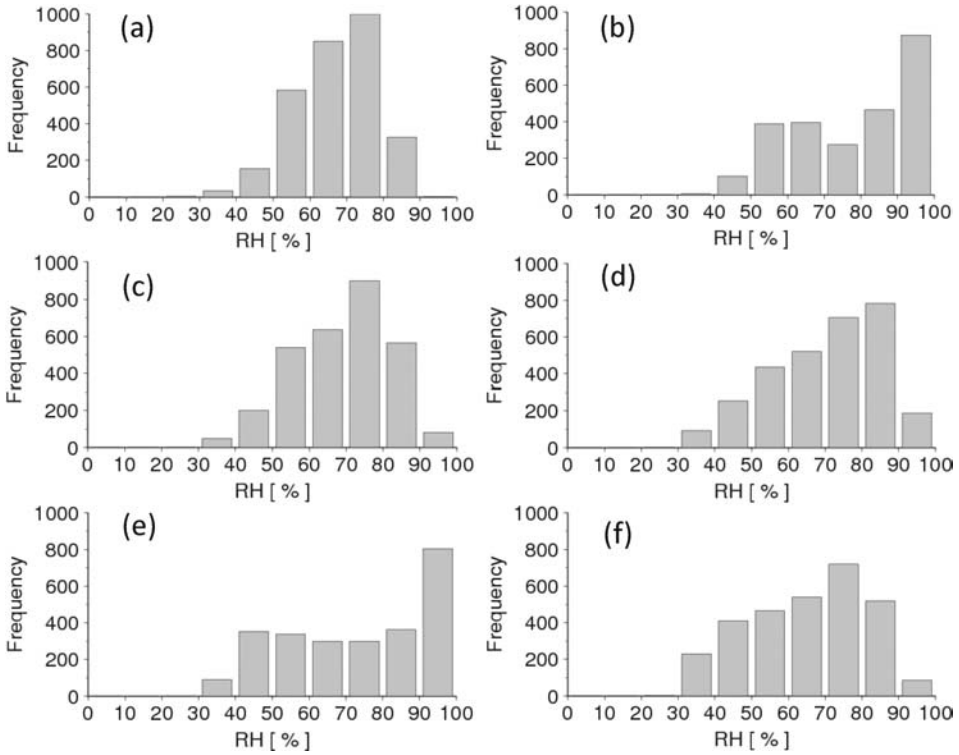

Fig. 10. Frequency of relative humidity. (a) AMeDAS observations, (b) SLAB, and (c) UCM at Tokyo. (d) AMeDAS observations, (e) SLAB, and (f) UCM at Kumagaya.

Table 6. Model bias of relative humidity [%] at the JMA observatories. RMSE values are in parentheses. TO, KU, MA, TS, UT, CHO, CHI, TA, and YO are city locations described in Table A1.

	TO	KU	MA	TS	UT	CHO	CHI	TA	YO
SLAB	+14.7	+7.7	+7.3	+1.4	+5.2	−2.8	+0.9	+7.5	+13.1
	(19.2)	(15.0)	(15.4)	(10.2)	(13.4)	(9.2)	(11.2)	(10.0)	(15.2)
UCM	+2.2	−4.7	−5.6	−2.4	−4.8	−10.7	−4.6	+3.7	+11.6
	(7.8)	(10.1)	(10.9)	(8.1)	(10.2)	(13.2)	(10.9)	(7.3)	(14.2)

Table A1. Full name of city and location for abbreviation codes used in Tables 5 and 6.

Code	Name	Latitude [°]	Longitude [°]
TO	Tokyo	35.690	139.760
KU	Kumagaya	36.150	139.380
MA	Maebashi	36.405	139.060
TS	Tsukuba	36.057	140.125
UT	Utsunomiya	36.548	139.868
CHO	Chosi	35.738	140.857
CHI	Chichibu	35.990	139.073
TA	Tateyama	34.987	139.865
YO	Yokohama	35.438	139.652

SLAB (Figs. 10d–f). As a result, SLAB exhibits both a larger bias and larger RMSE when compared to UCM results (Table 6). Whereas SLAB has a bias of +14.7% and RMSE of 19.2%, UCM produces better results with a bias of +2.2% and a RMSE of 7.8%. Moreover, UCM produces a lower RMSE at the other sites (Table 6), although the bias depends on the location, just as it does for the temperature data.

4. Discussion

A key finding of this study is that the UCM produced a nocturnal UHI, but SLAB did not. The reason for this difference can be seen by looking

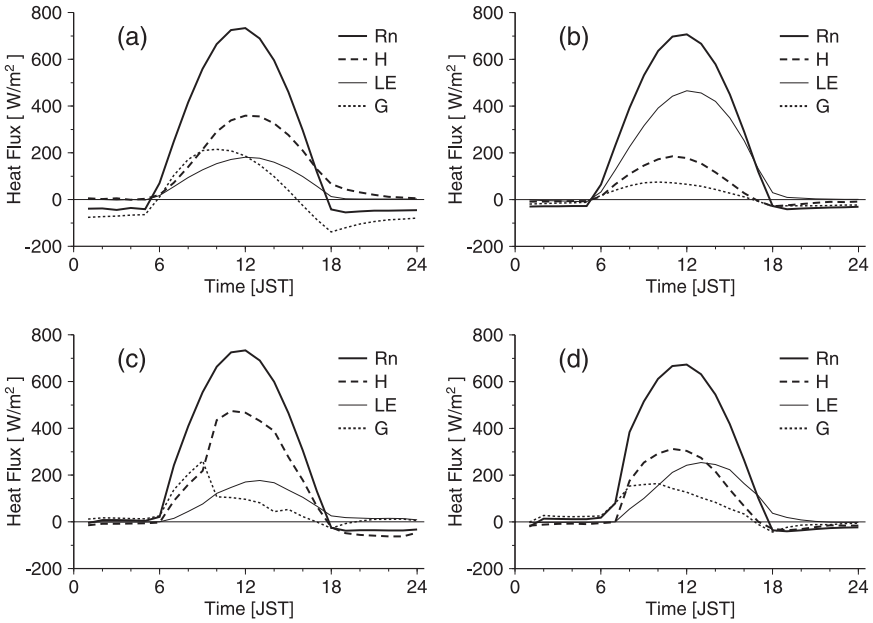

Fig. 11. Surface heat budget on a typical clear-sky day. (a) Tokyo and (b) Tsukuba from UCM. (c) Tokyo and (d) Tsukuba from SLAB.

at the heat budgets. For example, Figs. 11a,b show the surface energy budgets in UCM for an urban grid cell (Tokyo) and a rural grid cell (Tsukuba). A major difference between these two model grid cells is that the latent heat flux is much smaller during the daytime at Tokyo, indicating that the urban surface has less moisture than the rural surface due to the smaller amount of grassland. Another difference is that the heat storage is much larger during the daytime at Tokyo, and thus the sensible heat flux remains positive until midnight at the warmer urban surface. The duration of the heating depends on a number of factors, including the urban geometry, location, weather, and human activity. However, a positive sensible heat flux around sunset is an essential feature of an urban surface heat budget (e.g., Grimmond and Oke 1995; Sugawara et al. 2001). But SLAB does not show a positive sensible heat flux around sunset (Fig. 11c). Unlike the UCM case, the heat budget around sunset for SLAB is similar for Tokyo and Tsukuba (Figs. 11c,d). Another important difference between the two models is the larger ground-heat flux in the UCM model. According to numerical experiments with the single-layer UCM, the larger ground heat flux of the UCM arises from the walls of the urban area, which increase the effective thermal inertia, minimize the phase shift, decrease the diurnal temperature range, and increase the nocturnal temperature, especially around sunrise (Kusaka et al. 2001; Kusaka and Kimura 2004b). These effects occur even if the UCM and SLAB models have the same material thermal inertia. Moreover, a smaller sky view factor, due to existence of these walls, causes trapping of the reflected short- and long-wave radiation, and also reduces the temperature cooling especially around sunset. Thus, these previous findings indicate that the differences in the diurnal variation of temperature between UCM and SLAB in the present study arise from not only the differences in surface parameter values and anthropogenic heating, but also from the above urban canopy effects.

Finally, heat indices such as the discomfort index (temperature-humidity index), wet-bulb globe temperature (e.g., Tonouchi et al. 2006, Ohashi et al. 2008), and moist enthalpy (e.g., Pielke et al. 2006) are useful for predicting and analyzing heat stress and/or heat wave phenomenon. We plan to evaluate these indices in a future study.

5. Conclusions

In this study, we numerically simulated the urban heat island (UHI) effect and relative humidity (RH) in the WRF model coupled with the single-

layer urban canopy model (UCM) for four consecutive Augusts (2004–2007) in the Tokyo metropolitan area. We compared observations and results using the simpler SLAB land surface model with a different treatment of urban geometry and anthropogenic heat emission. We found the following.

(1) The WRF model with UCM well captures the observed monthly mean daytime and nocturnal UHI, but the WRF with SLAB did not show a nocturnal UHI. The surface air temperature bias, compared to observations, averaged over the entire analysis domain was −0.4°C for UCM and −0.6°C for SLAB, whereas their RMSE were 2.1 and 2.5°C, respectively.
(2) The observed diurnal variations of the surface air temperature at Tokyo and Kumagaya were also reproduced very well by UCM, but not by SLAB. Case SLAB had both a 1-hr phase shift and a 6.2°C larger diurnal range when compared to observations.
(3) Regarding the frequency distribution of the surface air temperature at Tokyo, UCM reproduced observations much better than SLAB. Both UCM and observations had a maximum frequency at approximately 27°C, whereas SLAB was bimodal, with peaks around 23 and 33°C. The bias for UCM and SLAB were +0.1 and −0.9°C, respectively. The RMSE for UCM and SLAB were 1.3 and 3.1°C, respectively.
(4) The improved bias, RMSE, correlation coefficients, phase error, and frequency distribution for the surface temperatures from UCM over SLAB lead to an advantage for derived temperature index quantities.
(5) UCM also reproduced the observed relative humidity better than SLAB.

The results from this report indicate that in the WRF model, the UCM model is more useful as an urban surface model than SLAB, not only for a case study of UHI but also for a dynamic downscaling study regarding the past/present urban climate simulation and future projections of urbanization.

Acknowledgements

This work was supported by the Global Environment Research Fund (S-5) of the Ministry of the Environment, Japan. Numerical simulations for the present work have been done under the ''Interdisciplinary Computational Science Program'' in the Center for Computational Sciences, University of Tsukuba. Free software 'GMT' (the Generic Mapping Tools) was used in drawing the figures.

References

Aoyagi, T., and N. Seino, 2011: A square prisom urban canopy scheme for the NHM and its evaluation on summer conditions in the Tokyo metrolpolitan area, Japan. *J. Appl. Meteor.*, **50**, 1476–1496.

Best, M. J., 2005: Representing urban areas within operational numerical weather prediction models. *Bound.-Layer Meteor.*, **88**, 279–306.

Brown, M., and M. Williams, 1998: An urban canopy parameterization for mesoscale meteorological models. Proc. of 2nd AMS Urban Environmental Symposium, Albuquerque, New Mexico, November 2–7, 1998, American Meteorological Society.

Castro, C. L., R. A. Pielke Sr., and G. Leconcini, 2005: Dynamical downscaling: Assessment of value retained and added using the Regional Atmospheric Modeling System (RAMS). *J. Geophys. Res.*, **110**, D05108, doi:10.1029/2004JD004721.

Chen, F., and J. Dudhia, 2001: Coupling an advanced land-surface/hydrology model with the Penn State/NCAR MM5 modeling system. Part I: Model implementation and sensitivity. *Mon. Wea. Rev.*, **129**, 569–585.

Chen, F., H. Kusaka, R. Bornstein, J. Ching, C. S. B. Grimmond, S. Grossman-Clarke, T. Loridan, K. W. Manning, A. Martilli, S. Miao, D. Sailor, F. P. Salamanca, H. Taha, M. Tewari, X. Wang, A. A. Wyszogrodzki, and C. Zhang, 2010: The integrated WRF/urban modeling system: Development, evaluation, and applications to urban environmental problems. *Int. J. Climatol.*, **31**, 273–288.

Chen, F., S. Miao, M. Tewari, J. Bao, and H. Kusaka, 2011: A numerical study of interactions between surface forcing and sea breeze circulations and their effects on stagnation in the greater Houston area. *J. Geophys. Res.*, **116**, D12105, doi:10.1029/2010JD015533.

Dandou, A., M. Tombrou, E. Akylas, N. Soulakellis, and E. Bossioli, 2005: Development and evaluation of an urban parameterization scheme in the Penn State/NCAR Mesoscale Model (MM5). *J. Geophys. Res.*, **110**, D10102, doi:10.1029/2004JD005192.

Dudhia, J., 1989: Numerical study of convection observed during the winter monsoon experiment using a mesoscale two-dimensional model. *J. Atmos. Sci.*, **46**, 3077–3107.

Dupont, S., T. L. Otte, and J. K. S. Ching, 2004: Simulation of meteorological fields within and above urban and rural canopies with a mesoscale model (MM5). *Bound.-Layer Meteor.*, **113**, 111–158.

Fire and Disaster Management Agency of Japan, 2011:

http://www.fdma.go.jp/neuter/topics/fieldList9_2.html (in Japanese).

Fujibe, F., 2009: Detection of urban warming in recent temperature trends in Japan. *Int. J. Climatol.*, **29**, 1811–1822.

Goto, K., K. Yabe, and N. Araki, 2004: Estimation of maximum demand sensitivity to the temperature for long-term power demand forecast. *Proc. Technical Meeting of Power and Energy Division 2004*, The Institute of Electrical Engineers of Japan, 13–21 (in Japanese).

Grimmond, C. S. B., and T. R. Oke, 1995: Comparison of heat fluxes from summertime observations in the suburbs of four North American cities. *J. Appl. Meteor.*, **34**, 873–889.

Grossman-Clarke, S., J. A. Zehnder, T. Loridan, and C. S. B. Grimmond, 2010: Contribution of land use changes to near-surface air temperatures during recent summer extreme heat events in the Phoenix metropolitan area. *J. Appl. Meteor. Climatol.*, **49**, 1649–1664.

Harman, I. N., J. F. Barlow, and S. E. Belcher, 2004: Scalar fluxes from urban street canyons. Part 2: Model. *Bound.-Layer Meteor.*, **113**, 387–410.

Holt, T., and J. Pullen, 2007: Urban canopy modeling of the New York city metropolitan area: A comparison and validation of single- and multilayer parameterizations. *Mon. Wea. Rev.*, **135**, 1906–1930.

Hong, S.-Y., and H.-L. Pan, 1996: Nonlocal boundary layer vertical diffusion in a medium-range forecast model. *Mon. Wea. Rev.*, **124**, 2322–2339.

Hong, S.-Y., J. Dudhia, and S.-H. Chen, 2004: A revised approach to ice microphysical processes for the bulk parameterization of clouds and precipitation. *Mon. Wea. Rev.*, **132**, 103–120.

Hong, S.-Y., Y. Noh, and J. Dudhia, 2006: A new vertical diffusion package with an explicit treatment of entrainment processes. *Mon. Wea. Rev.*, **134**, 2318–2341.

IAUC, 2009: Proceedings of the 7th International Conference on Urban Climate (ICUC-7), Yokohama, Japan. June 29–July 3, 2009.

Ihara, T., H. Kusaka, M. Hara, R. Matsuhashi, and Y. Yoshida, 2011: Estimation of mild health disorder caused by urban air temperature increase with midpoint-type impact assessment methodology. *J. Environ. Eng., AIJ*, **76**, 459–467 (in Japanese with an English abstract).

Ikeda, R., and H. Kusaka, 2009: Proposing the simplification of the multilayer urban canopy model: Intercomparison study of four models. *J. Appl. Meteor.*, **49**, 902–919.

Jiang, X., C. Wiedinmyer, F. Chen, Z.-L. Yang, and J. C.-F. Lo, 2008: Predicted impacts of climate and land use change on surface ozone in the Houston, Texas, area. *J. Geophys. Res.*, **113**, D20312, doi:10.1029/2008JD009820.

Kain, J. S., and J. M. Fritsch, 1990: A one-dimensional entraining/detraining plume model and its application in convective parameterization. *J. Atmos. Sci.*, **47**, 2784–2802.

Kain, J. S., 2004: The Kain-Fritsch convective parameterization: An update. *J. Appl. Meteor.*, **43**, 170–181.

Kanda, M., T. Kawai, M. Kanega, R. Moriwaki, K. Narita, and A. Hagishima, 2005: A simple energy balance model for regular building arrays. *Bound.-Layer Meteor.*, **116**, 423–443.

Kimura, F., 1989: Heat flux on mixtures of different land-use surface: Test of a new parameterization scheme. *J. Meteor. Soc. Japan*, **67**, 410–409.

Kondo, H., Y. Genchi, Y. Kikegawa, Y. Ohashi, H. Yoshikado, and H. Komiyama, 2005: Development of a multi-layer urban canopy model for the analysis of energy consumption in a big city: Structure of the urban canopy model and its basic performance. *Bound.-Layer Meteor.*, **116**, 395–421.

Kusaka, H., and F. Kimura, 2004a: Coupling a single-layer urban canopy model with a simple atmospheric model: Impact on urban heat island simulation for an idealized case. *J. Meteor. Soc. Japan*, **82**, 67–80.

Kusaka, H., and F. Kimura, 2004b: Thermal effects of urban canyon structure on the nocturnal heat island: Numerical experiment using mesoscale model coupled with urban canopy model. *J. Appl. Meteor.*, **43**, 1899–1910.

Kusaka, H., H. Kondo, Y. Kikegawa, and F. Kimura, 2001: A simple single-layer urban canopy model for atmospheric models: Comparison with multi-layer and slab models. *Bound.-Layer Meteor.*, **101**, 329–358.

Landsberg, H. E., 1981: The urban climate. Academic press, 269 pp.

Lee, S., and S. Park, 2008: A vegetated urban canopy model for meteorological and environmental modeling. *Bound.-Layer Meteor.*, **126**, 73–102.

Lemonsu, A., and V. Masson, 2002: Simulation of a summer urban breeze over Paris. *Bound.-Layer Meteor.*, **104**, 4630–490.

Lin, C., F. Chen, J. C. Huang, W. Chen, Y. Liou, W. Chen, and S. Liu, 2008: Urban heat island effect and its impact on boundary layer development and land-sea circulation over northern Taiwan. *Atmos. Environ.*, **42**, 5635–5649.

Lin, C., W. Chen, P. Chang, and Y. Sheng, 2011: Impact of the urban heat island effect on precipitation over a complex geographic environment in northern Taiwan. *J. Appl. Meteor. Climatol.*, **50**, 339–353.

Liu, C., K. Ikeda, G. Thompson, R. Rasmussen, and J. Dudhia, 2011: High-resolution simulations of

wintertime precipitation in the Colorado Headwaters region: sensitivity to physics parameterizations. *Mon. Wea. Rev*. doi:10.1175/MWR-D-11-00009.1, in press.

Martilli, A., A. Clappier, and M. W. Rotach, 2002: An urban surface exchange parameterization for mesoscale models. *Bound.-Layer Meteor*., **104**, 261–304.

Masson, V., 2000: A physically-based scheme for the urban energy budget in atmospheric models. *Bound.-Layer Meteor*., **94**, 357–397.

McCarthy, M. P., M. J. Best, and R. A. Betts, 2010: Climate change in cities due to global warming and urban effects. *Geophy. Res. Lett.*, **37**, L09705, doi:10.1029/2010GL042845.

Miao, S., F. Chen, M. A. LeMone, M. Tewari, Q. Li, and Y. Wang, 2009: An observational and modeling study of characteristics of urban heat island and boundary layer structures in Beijing. *J. Appl. Meteor. Climatol.*, **48**, 484–501.

Miao, S., F. Chen, Q. Li, and S. Fan, 2010: Impacts of urban processes and urbanization on summer precipitation: A case study of heavy rainfall in Beijing on 1 August 2006. *J. Appl. Meteor. Climatol.*, **50**, 806–825.

Miao, S., F. Chen, Q. Li, and S. Fan, 2011: Month-averaged impacts of urbanization on atmospheric boundary layer structure and precipitation in summer in Beijing area. *Chinese J. Geophys.—Chinese Edition*, **53**, 1580–1593.

Mlawer, E. J., S. J. Taubman, P. D. Brown, M. J. Iacono, and S. A. Clough, 1997: Radiative transfer for inhomogeneous atmosphere: RRTM, a validated correlated-*k* model for the longwave. *J. Geophys. Res.*, **102** (D14), 16663–16682.

Ohashi, Y., T. Kawabe, Y. Shigeta, Y. Hirano, H. Kusaka, H. Fudeyasu, and K. Fukao, 2008: Evaluation of urban thermal environments in commercial and residential spaces in Okayama city, Japan, using the wet-bulb globe temperature index. *Theor. Appl. Climatol.*, doi: 10.1007/s00704-008-0006-8.

Oke, T. R., 1987: Boundary layer climate 2nd edition. Methuen Co., 433 pp.

Oleson, K. W., G. B. Bonan, J. Feddema, M. Vertenstein, and C. S. B. Grimmond, 2008: An urban parameterization for a global climate model. 1. Formulation and evaluation for two cities. *J. Appl. Meteor. Climatol*., **47**, 1038–1060.

Oleson, K. W., G. B. Bonan, J. Feddema, and T. Jackson, 2011: An examination of urban heat island characteristics in a global climate model. *Int. J. Climatol.*, in press.

Otte, T. L., A. Lacser, S. Dupont, and J. K. S. Ching, 2004: Implementation of an urban canopy parameterization in a mesoscale meteorological model. *J. Appl. Meteor.*, **43**, 1648–1665.

Pielke, R. A. Sr., K. Wolter, O. Bliss, N. Doesken, and B. McNoldy, 2006: The July 2005 Denver heat wave: How unusual was it? *National Weather Digest*, **31**, 24–35.

Porson, A., I. N. Harman, S. Bohnenstengel, and S. E. Belcher, 2009: How many facets are needed to represent the surface energy balance of an urban area? *Bound.-Layer Meteor.*, **132**, 107–128.

Porson, A., P. A. Clark, I. N. Harman, M. J. Best, and S. E. Belcher, 2010: Implementation of a new urban energy budget scheme in the MetUM. Part I: Descripition and idealzed simulations. *Q. J. Roy. Meteor. Soc.*, **136**, 1514–1529.

Rozoff, C. M., W. R. Cotton, and J. O. Adegoke, 2003: Simulation of St. Louis, Missouri, land use impacts on thunderstorms. *J. Appl. Meteor.*, **42**, 716–738.

Shou, Y., and D. Zhang, 2010: Impact of environmental flows on the daytime urban boundary layer structures over the Baltimore metropolitan region. *Atmospheric Science Letters*, **11**, 1–6.

Skamarock, W. C., J. B. Klemp, J. Dudhia, D. O. Gill, D. M. Barker, M. G. Duda, X.-Y. Huang, W. Wang, and J. G. Powers, 2008: A description of the advanced research WRF version 3, NCAR/TN-475+STR, 126 pp.

Sugawara, H., 2001: Heat exchange between urban structures and the atmospheric boundary layer. Ph.D. thesis, Tohoku University, 140 pp.

Takane, Y., and H. Kusaka, 2011: Formation mechanisms of the extreme high surface air temperature of 40.9°C observed in the Tokyo metropolitan area: Considerations of dynamic foehn and foehn-like wind. *J. Appl. Meteor. Climatol.*, **50**, 1827–1841.

Tewari, M., H. Kusaka, F. Chen, W. J. Coirier, S. Kim, A. A. Wyszogrodzki, and T. T. Warner, 2010: Impact of coupling a microscale computational fluid dynamics model with a mesoscale model on urban scale contaminant transport and dispersion. *Atmos. Res.*, **96**, 656–664.

Tonouchi, M., K. Maruyama, and M. Ono, 2006: WBGT forecast for prevention of heat stroke in Japan. Sixth Symposium on the urban environment, American Meteorological Society, session PJ1.1.

Yoshino, M., 1975: Climate in a small area. University of Tokyo press, 549 pp.

Zhang, H., N. Sato, T. Izumi, K. Hanaki, and T. Aramaki, 2007: Modified RAMS-Urban canopy model for heat island simulation in Chongqing, China. *J. Appl. Meteor. Climatol.*, **47**, 509–524.

Zhang, N., G., Z. Gao, X. Wang, and Y. Chen, 2010: Modeling the impact of urbanization on the local and regional climate in Yangtze River Delta, China. *Theor. Appl. Climatol.*, **102**, 331–341.